THE JOURNAL OF BIOLOGICAL CHEMISTRY VOL. 281, NO. 32, pp. 22964–22973, August 11, 2006

The Role of the STAS Domain in the Function and Biogenesis of a Sulfate Transporter as Probed by Random Mutagenesis*

Received for publication, April 11, 2006, and in revised form, June 2, 2006 Published, JBC Papers in Press, June 5, 2006, DOI 10.1074/jbc.M603462200

Nakako Shibagaki[1] **and Arthur R. Grossman**

From the Department of Plant Biology, The Carnegie Institution, Stanford, California 94305

Sulfate transporters in plants represent a family of proteins containing transmembrane domains that constitute the catalytic part of the protein and a short linking region that joins this catalytic moiety with a C-terminal STAS domain. The STAS domain resembles an anti-sigma factor antagonist of *Bacillus subtilis*, which is one distinguishing feature of the SLC26 transporter family; this family includes transporters for sulfate and other anions such as iodide and carbonate. Recent work has demonstrated that this domain is critical for the activity of *Arabidopsis thaliana* sulfate transporters, and specific lesions in this domain, or the exchange of STAS domains between different sulfate transporters, can severely impair transport activity. In this work we generated a *Saccharomyces cerevisiae* expression library of the *A. thaliana Sultr1;2* gene with random mutations in the linking region-STAS domain and identified STAS domain lesions that altered Sultr1;2 biogenesis and/or function. A number of mutations in the β-sheet that forms the core of the STAS domain prevented intracellular accumulation of Sultr1;2. In contrast, the linking region and one surface of the STAS domain containing N termini of the first and second α-helices have a number of amino acids critical for the function of the protein; mutations in these regions still allow protein accumulation in the plasmamembrane, but the protein is no longer capable of efficiently transporting sulfate into cells. These results suggest that the STAS domain is critical for both the activity and biosynthesis/stability of the transporter, and that STAS sub-domains correlate with these specific functions.

Sulfate transporters, designated Sultr (*Sultr* for the gene) in plants, are part of the SLC26 family of anion transporters that also includes iodide, chloride, and carbonate transporters and the motor protein prestin, which resides in the outer hair cells of the cochlea (1). SLC26 family proteins are predicted to have ten to fourteen transmembrane domains (TMDs)[2] and a C-terminal extension, designated as the STAS domain (2), that protrudes into the cytosol of the cell (3, 4). The STAS domain is joined to the catalytic domain of transporters by a linking (L) region, varies in length, and is not highly conserved relative to the catalytic domain. Some characteristics that make SLC26 transporters distinct from each other are likely to reside within unique features of L-STAS domains.

Interestingly, the STAS domain of SLC26 transporter proteins resembles the bacterial anti-sigma factor antagonist SpoIIAA of *Bacillus* (2). SpoIIAA is a transcription factor that associates with the anti-sigma factor SpoIIAB; this association causes release of the sigma factor from SpoIIAB, triggering sporulation-specific transcription (5). SpoIIAB is also a kinase that can phosphorylate and inactivate SpoIIAA. Recently, STAS domains have been shown to be part of polypeptides other than anion transporters (6), suggesting that STAS sequences may serve a general regulatory function.

STAS domains of SLC26 transporters appear to play a role in the function/regulation of transport activity, because mutations that alter this domain can cause loss of function resulting in the diseases diastrophic dysplasia, Pendred syndrome, and congenital chloride diarrhea (7–12). Recent work, using a heterologous *Saccharomyces cerevisiae* system, has demonstrated that the STAS domain is critical for the activity of the *Arabidopsis thaliana* sulfate transporter Sultr1;2 (13, 14). When the L-STAS region of the sulfate transporter was eliminated, most of the truncated protein either never reached the *S. cerevisiae* plasmamembrane and was rapidly degraded, either en route to or once associated with the plasmamembrane. In contrast, if the STAS domain was deleted (L region maintained), the transporter integrated into the plasmamembrane, but the integrated protein had no detectable uptake activity. Studies of the DRA (down-regulated in adenoma) Cl^--HCO_3^- antiporter (SLC26A3) also demonstrated a STAS domain requirement for transport function (15). Furthermore, altering *A. thaliana* Sultr1;2 for codons encoding two cysteines or a threonine of the STAS domain (the latter is analogous to the phosphorylated serine of SpoIIAA) resulted in a polypeptide no longer able to rescue the phenotype of a *S. cerevisiae* sulfate transporter mutant (14). These results suggest that the STAS domain contributes to both the catalytic activity and biogenesis of Sultr1;2 and probably has analogous functions in other SLC26 proteins.

The control of ion homeostasis in cells is likely to involve interactions among transporters, ion channels, regulatory proteins, proteins involved in ion assimilation and sequestration, and concentrations of ions and perhaps other small molecules in the cytoplasm and/or extracellular environment. For SLC26 family proteins, the STAS domain appears to participate in some aspects of homeostatic control. Recent studies with the

* This work was supported by United States Department of Agriculture Grants 2003-35100-13235 (to A. R. G.) and by the Japan Society for the Promotion of Science (to N. S.). This is a Carnegie Institution Publication (No. 1677). The costs of publication of this article were defrayed in part by the payment of page charges. This article must therefore be hereby marked "*advertisement*" in accordance with 18 U.S.C. Section 1734 solely to indicate this fact.

[1] To whom correspondence should be addressed: Dept. of Plant Biology, Carnegie Institution, 260 Panama St., Stanford, CA 94305. Tel.: 650-325-1521 (ext. 241); Fax: 650-325-6857; E-mail: snakako@stanford.edu.

[2] The abbreviations used are: TMD, transmembrane domain; L region, linking region; DRA, down-regulated in adenoma; HA, hemagglutinin; DTDST, diastrophic dysplasia sulfate transporter; A_{600}, optical density at 600 nm; Pma1, plasmamembrane H^+-ATPase 1.

DRA Cl^--HCO_3^- antiporter have demonstrated the importance of STAS domain interactions with the regulatory sequence of the cystic fibrosis transmembrane conductance regulator, a cAMP-regulated Cl^- channel. This interaction modulates the activity of both the transporter and the channel (16).

To elucidate protein domain function, the generation and characterization of mutants can be invaluable. *S. cerevisiae* has served as a heterologous expression system for many eukaryotic genes, and mutant strains have been used to study the catalytic activity and kinetic features of several plant sulfate transporters (13, 14, 17–20). In this study we generated a yeast expression library of the *A. thaliana Sultr1;2* gene that had random mutations in the L-STAS domain and selected individual, mutated *Sultr1;2* genes by transforming them into CP154-7B, which is null for the two major *S. cerevisiae* sulfate transporters (21). Transformants were analyzed for their ability to grow on SO_4^{2-} as a sole sulfur (S) source, ability to transport SO_4^{2-}, and capacity to accumulate the altered Sultr1;2 polypeptide and properly target it to the plasmamembrane. Lesions in the L-STAS-encoding region of altered *Sultr1;2* were characterized to determine which amino acids were critical to the functionality/biogenesis of the Sultr1;2 polypeptide. The consequences of mutations in the STAS domain are discussed and interpreted with the aid of a computer-derived structural model based on the crystal structure of SpoIIAA (14, 22).

EXPERIMENTAL PROCEDURES

Yeast Strains

The *S. cerevisiae* strain used in this study was CP154-7B (*MATα*, *ade2*, *his3*, *leu2*, *trp1*, *ura3*, *sul1*:*LEU2*, *sul2*:*URA3*), which is null for both the *Sul1* and *Sul2* sulfate transporter genes (21).

Construction and Screening of a Library of Sultr1;2 Containing Random Mutations in the STAS Domain

Intermediate Construct (pIMRNDM)—Plasmids used for expression of the C-terminal, hemagglutinin (HA)-tagged sulfate transporters were constructed in pYX222x (13) (Fig. 1*A*). This plasmid (a) was digested with EcoRI and BamHI and the resulting linearized vector (a′) in which the region encoding the catalytic domain plus part of the region encoding the L-STAS domain (to the BamHI site) was deleted. The deleted plasmid was ligated with a PCR-amplified EcoRI-BamHI fragment containing the sequence encoding Sultr1;2, extending from the initiator Met-1 to Phe-478 (the end of the catalytic region; this fragment is designated "*b*" in Fig. 1*A*). The primer set used to create b was forward (5′-ata *gaa ttc* atg tcg tca aga gct cac cct gtg gac-3′) and reverse (5′-ata *gga tcc* aaa gat gac gcc aaa gaa tgc tcc aat-3′). The resulting intermediate construct, pIMRNDM, was used to clone a randomly mutagenized L-STAS encoding region. For this purpose, we introduced a BamHI site at nucleotides 1495–1500 in the *Sultr1;2* cDNA (GenBank™ accession no. AB042322), which resulted in a V479G substitution in TMD12 of the catalytic region of the transporter. This amino acid is not conserved among *S. cerevisiae*, plant, and human SLC26 family members (it could be Val, Leu, Gly, Ala, Ile, or Phe), and this region of the C-terminal TMD does not appear to directly influence substrate transport.

Construction of Sultr1;2 Library with Mutated STAS Domains—During the amplification of the *Sultr1;2* cDNA, we identified an allele of the *Sultr1;2* gene with the missense mutation I553V (a to g at position 1717) that arose as a consequence of the natural error rate of TaqDNA polymerase. This mutation eliminated the BamHI site in the *Sultr1;2* cDNA. The CP154-7B strain transformed with the allele containing V479G/I553V (WT′) was rescued for the methionine auxotrophy phenotype and exhibited SO_4^{2-} transport activity similar to that of CP154-7B harboring the unaltered *Sultr1;2* gene (WT, Fig. 1*B*). The *Sultr1;2* cDNA encoding the I553V lesion was used as a template for PCR random mutagenesis; this enabled us to exploit the BamHI sites at the N-terminal end of the L-STAS domain for digesting (with BamHI/SalI) and cloning of PCR fragments into pIMRNDM deleted for the L-STAS region of Sultr1;2. Random mutagenesis of the L-STAS encoding region was performed by PCR amplification of the cDNA using the DiversityKit (Clontech, Palo Alto, CA) and the primer set RNDMFB (5′-ata *gga tcc* gtt gag atc gga ctt ctt att gcc gtc tcg-3′) and RNDMRS (5′-act aa*g tcg ac*c gac ctc gtt gga gag ttt tgg aca gca-3′). Two conditions with different $MnSO_4$ concentrations (320 μM and 640 μM, for "mild" and "severe" mutagenesis, respectively) were used to generate the mutagenized libraries. The mildly mutagenesis library had 2–3 mutation per 1000 bp, whereas the severely mutagenized library had 4–6 mutations per 1000 bp. The PCR fragment of the mutated L-STAS region ("*e*" in Fig. 1*A*) was digested with BamHI and SalI and cloned into pIMRNDM digested with the same enzymes ("*c*′" in Fig. 1*A*).

Selection and Growth of Transformants—The cDNA L-STAS-mutagenized library was transformed into CP154-7B by the lithium acetate method (23), and transformants were selected for histidine auxotrophy. Each transformant was streaked onto low SO_4^{2-} SD medium (500 μM SO_4^{2-}, 400 μM methionine, and 96 μM histidine) and high SO_4^{2-} SD medium (40 mM SO_4^{2-}, 143 μM methionine, and 96 μM histidine) to test for SO_4^{2-}-dependent growth. Growth of the transformants was monitored at 30 °C for 2–3 days. DNA fragments coding for the L-STAS domains of the various *Sultr1;2* alleles were amplified by colony PCR using a primer set that annealed to sequences bordering the L-STAS-encoding region (forward, 5′-c atc ctc gca gct atc atc at-3′ and reverse, 5′-ctc agt tag cta gct gag-3′), and the amplified fragment was sequenced.

Growth, Subcellular Location, and Sulfate Uptake

CP154-7B transformants were grown at 30 °C in SD-His-Met liquid medium, containing 500 μM $MgSO_4$, or SD-His liquid medium, containing ~40 mM SO_4^{2-}. Transformants were assayed for rates of growth, SO_4^{2-} transport activity, and subcellular location of Sultr1;2. Cell growth was evaluated by measuring the optical density of cultures at 600 nm (A_{600}) in a DU640 spectrophotometer (Beckman Coulter, Palo Alto, CA). Cells in mid-logarithmic phase of growth ($A_{600} = 0.2–0.3$) were used for fractionation of cell membranes and polypeptide analysis (13). SO_4^{2-} uptake was assayed in exponentially growing cells ($A_{600} < 0.4$) (13).

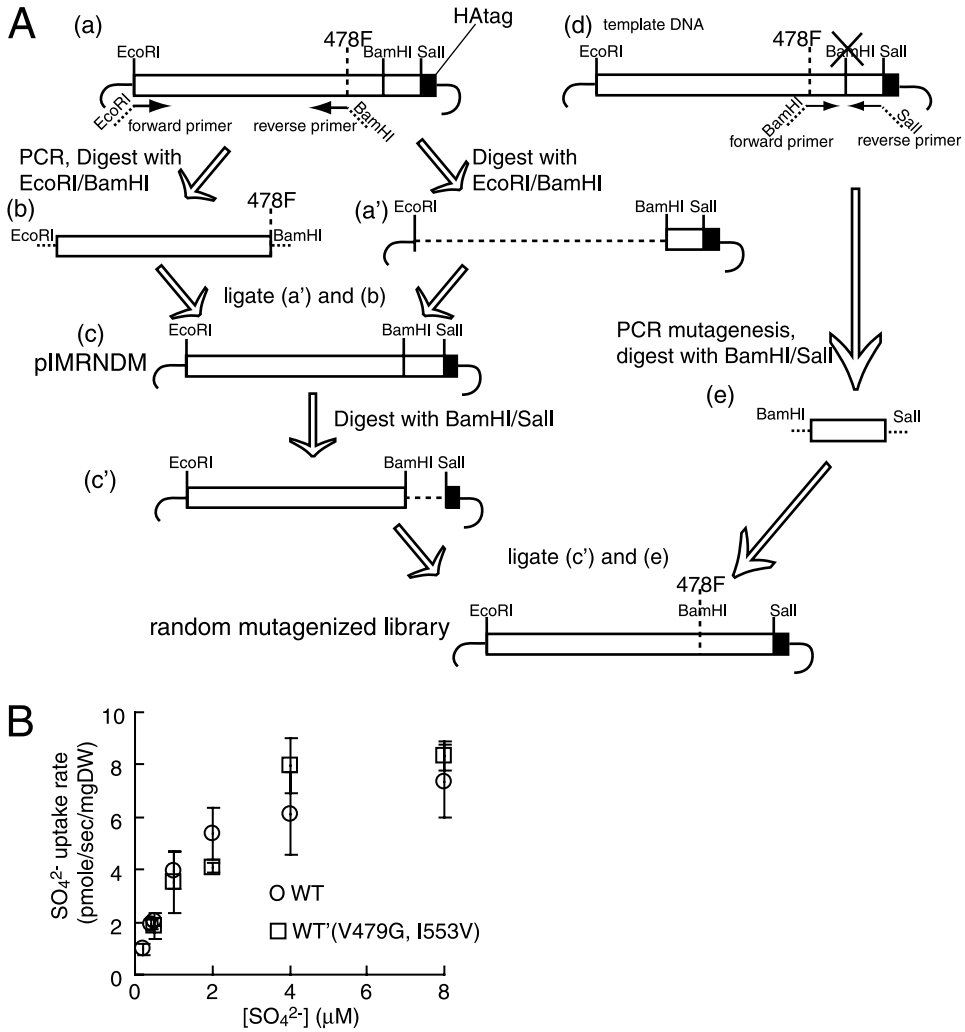

FIGURE 1. *A*, schematic of steps in the construction of the full-length *Sultr1;2* gene with random mutations in the L-STAS-encoding region. *a*, unaltered *Sultr1;2* cDNA in the vector pYX222x. *a'*, vector fragment from *a* after digestion with EcoRI and BamHI. *b*, PCR-amplified portion of *Sultr1;2* cDNA encoding Met-1 to Phe-478 (catalytic domain) digested with EcoRI and BamHI. *c*, pIMRNDM, intermediate plasmid generated by the ligation of *a'* and *b*. *c'*, vector fragment from *c* after digested with BamHI and SalI. *d*, same as *a* except for mutation from *a* to *c* at 1717 (GenBank™ accession number AB042322); this mutation eliminated a BamHI site in the STAS domain coding sequence. *e*, PCR-amplified fragment encoding the L-STAS domain (480S to 653V) with random mutations. Fragments *c'* and *e* were ligated to generate the library of *Sultr1;2* cDNA with random mutations in the L-STAS-encoding region. *B*, SO_4^{2-} uptake rate in CP154-7B cells expressing wild-type Sultr1;2 (*WT*) and Sultr1;2 with V479G and I553V mutations (*WT'*). Assays were performed as described under "Experimental Procedures," and uptake rates were normalized to dry weight (*DW*).

Polypeptide Analyses

Cells in mid-logarithmic growth phase (A_{600} = 0.2–0.3) were used for SDS-PAGE (13). Monoclonal antibodies raised to H^+-ATPase1 (Pma1), a plasmamembrane marker, were purchased from Abcam (Cambridge, MA), and anti-HA antibodies (Roche Applied Science) were used to detect the C-terminal HA-tagged Sultr1;2 polypeptide.

Alignments and Threading

SLC26 family proteins from humans (PENDRIN (O43511), DRA (P40879), prestin (P58743), and DTDST (P50443)), *A. thaliana* (Sultr1;1 (NP 192602), Sultr1;2 (NP 849899), Sultr2;1 (O04722), Sultr2;2 (NP565165), Sultr3;1 (NP190758), Sultr1;3 (NP564159), Sultr3;2 (NP192179), Sultr3;3 (BAA75015), Sultr3;4 (NP188220), Sultr3;5 (NP568377), Sultr4;1 (NP196859), and Sultr4;2 (NP187858); GenBank™ accession numbers are in parenthesis) and SpoIIAA from *Bacillus sphaericus* (PDB ID 1h4z) were aligned using ClustalW. Alignment parameters were gap opening penalty = 10, gap extension penalty = 0.2, delay divergent sequence = 30, and hydrophobic residue gap = GPSNDQEKR. The amino acid alignments of the C-terminal half of the Sultr1;2 polypeptide, which includes the L-STAS domain, are presented as a sequence logo (24) (available at weblogo.berkeley.edu/).

RESULTS

Generating Mutagenized L-STAS of Sultr1;2—Random mutations were introduced into the *Sultr1;2* sequence encoding the L-STAS domain (from the end of TMD12 to the end of the polypeptide; described under "Experimental Procedures"). The mutant *Sultr1;2* cDNA library was transformed into *S. cerevisiae* CP154-7B (21), and transformants were tested for methionine-independent, SO_4^{2-}-dependent growth on solid medium (Fig. 2*A*). This assay provided an evaluation of the effectiveness of the introduced *Sultr1;2* gene in rescuing the methionine auxotrophy phenotype of CP154-7B. *Sultr1;2* alleles carried by transformants unable to grow in the absence of methionine were mostly from the "mild condition" mutagenized library (except for alleles "Y517C+V616E," "N545I," and "S588R"), because the "severe condition"-mutagenized library often gave multiple mutations, making it difficult to interpret the phenotypes; these alleles were categorized as "nonfunctional." We also identified "functional" alleles in transformants for which the mutated Sultr1;2 was able to rescue the methionine auxotrophy phenotype of CP154-7B (Fig. 2*A*). These functional alleles were isolated using the severe condition mutagenized library, because the majority of changes in functional alleles identified from the mild mutagenesis library were silent (the amino acid sequence was not altered). Colony PCR was performed to amplify DNA fragments encoding the L-STAS domain of Sultr1;2 in transformants, and amplified fragments were directly sequenced to identify mutated bases. For nonfunctional mutants, only alleles containing a single missense mutation were chosen for further analyses, except for the allele with both Y517C and V616E substitutions. Table 1 shows specific changes in STAS domain

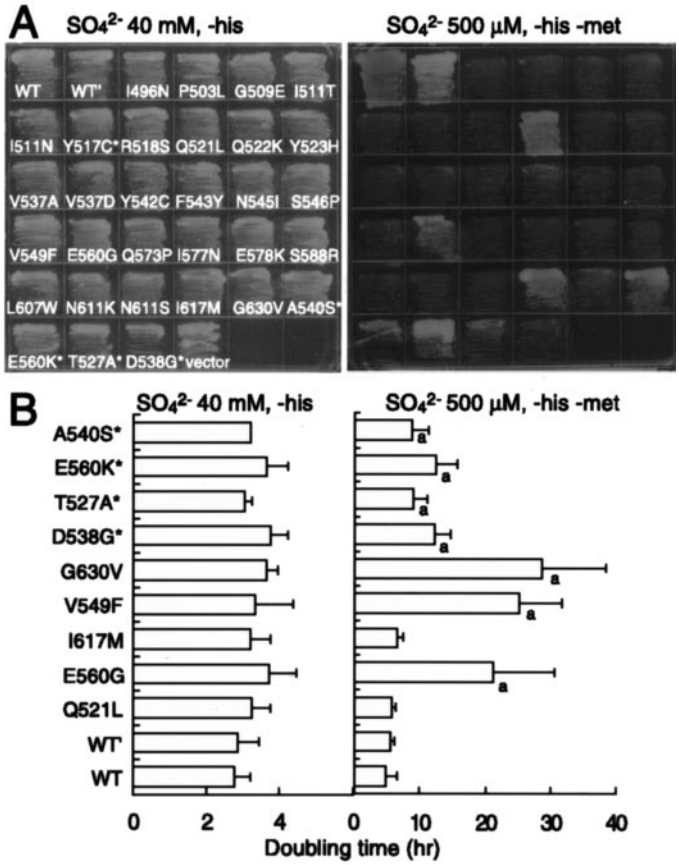

FIGURE 2. **Growth of CP154-7B harboring the unaltered *Sultr1;2* gene or *Sultr1;2* with random mutations in the L-STAS domain.** *A*, CP154-7B transformed with constructs harboring the unaltered *Sultr1;2* gene (*WT*), *Sultr1;2* with two mutations introduced for cloning purposes (*WT'*), mutated versions of *Sultr1;2*, and an empty vector plasmid (vector). The descriptions of amino acid changes caused by the introduced mutations are used as allele names. Mutant alleles marked with *asterisks* contain additional lesions. Transformed lines were grown on solid SD-His medium containing 40 mM SO_4^{2-} (*left panel*) or SD-His-Met medium containing 500 μM SO_4^{2-} (*right panel*), at 30 °C for 2 days. *B*, doubling times of CP154-7B expressing functional Sultr1;2 in liquid medium containing 40 mM and 500 μM SO_4^{2-}. The *bars*, representing the doubling time in wild-type and mutant strains, are marked with *a'* (at *end of bar*) when the growth rates were significantly different from those of WT' ($p < 0.02$, two-tailed Student's *t* test). The doubling time of each transformant is an average value obtained from at least three separate experiments.

sequences from transformants expressing functional or nonfunctional Sultr1;2, provides a qualitative view of accumulation of Sultr1;2 in cells, and indicates whether or not the transporter localizes to the plasmamembrane (see below). A DNA fragment encoding the L-STAS peptide from each mutant allele was recloned into pIMRNDM to generate full-length *Sultr1;2*, the ligated insert was sequenced to ensure that no modification occurred during the cloning procedure, and the plasmid with the recombinant gene was transformed into CP154-7B; re-transformation was performed to confirm that the phenotype was solely a consequence of a lesion in the L-STAS region of the polypeptide.

The previously characterized *A. thaliana sel1–3*, *sel1–7*, and *sel1–8* mutants have lesions in the L-encoding region of *Sultr1;2* (G509E, P503L, and I511T, respectively); these lesions make the plant resistant to selenate (27). SO_4^{2-} uptake rates in the *sel1–8* mutant of *A. thaliana* were reported to be lower than in the wild-type plants (27). None of these altered *Sultr1;2* alleles could rescue the methionine auxotrophy phenotype of CP154-7B, as shown in Fig. 2*A* (compare sulfate, 40 mM, with sulfate, 500 μM, in the *top row* of each grid). These mutant alleles do not have the lesions incorporated into the constructs for cloning purposes (V479G and I553V).

Phenotypic Analysis of S. cerevisiae Cells Expressing Sultr1;2—SO_4^{2-}-dependent growth characteristics of strains newly transformed with plasmids containing WT, WT′, and the randomly mutagenized *Sultr1;2* alleles were monitored for growth in high and low SO_4^{2-} medium. CP154-7B transformed with unaltered *Sultr1;2* or with the *Sultr1;2* allele with the V479G and I553V changes doubled in ~2.8 h in SD-His medium containing 40 mM SO_4^{2-} (high SO_4^{2-} medium, Fig. 2*B*, *left panel*, WT and WT′), which is close to that of wild-type *S. cerevisiae* cells (W303 cells, not shown). All nonfunctional transformants grew in high SO_4^{2-} medium with doubling times from 3 to 4 h (not shown). In most cases, growth rates were only slightly slower than that of cells harboring unaltered *Sultr1;2*. Although the doubling time of CP154-7B with unaltered *Sultr1;2* on low SO_4^{2-} medium was ~5 h (Fig. 2*B*, *right panel*, WT and WT′), all nonfunctional transformants showed no, or extremely slow growth in low SO_4^{2-} liquid medium (not shown). In contrast, doubling times of CP154-7B with functional *Sultr1;2* alleles ranged from 5 to nearly 30 h on low SO_4^{2-} medium (Fig. 2*B*, *right panel*), and from 3 to 4 h on high SO_4^{2-} medium (Fig. 2*B*, *left panel*).

Accumulation of Nonfunctional Sultr1;2—Sultr1;2 protein accumulation in nonfunctional transformants was evaluated in whole cell extracts by Western blot analyses using antibodies specific for the HA tag (positioned at the C terminus of the Sultr1;2 protein). The fusion of the HA epitope to the C terminus of the introduced protein does not affect the ability of Sultr1;2 to rescue the CP154-7B mutant phenotype (13). An antibody against Pma1 was used as a control to identify the plasmamembrane fraction and to normalize the HA signal. The level of the HA signal relative to that of Pma1 is shown in Fig. 3*A* and quantified in Fig. 3*B*. Some transformants with nonfunctional *Sultr1;2* had significantly less Sultr1;2 protein than cells transformed with WT′ *Sultr1;2*. Transformants for which the ratio of Sultr1;2 to Pma1 signal was 20% or less relative to that measured in transformants harboring the WT′ *Sultr1;2* construct were S546P, Q573P, I577N, E578K, and L607W. Low level protein accumulation in these strains is likely to explain their inability to grow on low SO_4^{2-} medium and to efficiently transport SO_4^{2-}; these mutant alleles are classified as Class I in Table 1.

Most transformants with nonfunctional Sultr1;2 had polypeptide levels similar to that of the WT′ transformant (Table 1; Class II). Some transformants for which the CP154-7B mutant phenotype was not rescued by the introduced *Sultr1;2* gene, even though the Sultr1;2 protein in these strains appeared to accumulate, may experience difficulties in routing the expressed polypeptide to its site of function on the plasmamembrane. In a previous study (28), a G678V mutation in the STAS domain of DTDST (SLC26A2) abolished plasmamembrane targeting of the protein. Therefore, we examined all transformants determined to have nonfunctional Sultr1;2, but that accumulated a range of Sultr1;2 levels, for distribution of

TABLE 1

Summary of mutations analyzed in this work

Class I includes alleles of the mutated *Sultr1;2* gene for which the protein accumulates to significantly lower levels (<20%) than that of the unaltered Sultr1;2 polypeptide but does not rescue the methionine auxotroph phenotype of CP154-7B. Class II includes alleles of mutated *Sultr1;2* gene for which the protein is expressed and accumulates in the plasmamembrane, but it does not rescue the methionine auxotroph phenotype of CP154-7B. Class III includes alleles of mutated *Sultr1;2* gene for which the protein confers varying SO_4^{2-} uptake activity to CP154-7B, but the transformants may not grow as rapidly in low SO_4^{2-} medium as CP154-7B transformed with the unaltered *Sultr1;2* gene. Complementation of the growth phenotype of CP154-7B on SO_4^{2-} is based on data shown in Fig. 2: −, no growth on SO_4^{2-}; + and ++, slow growth on SO_4^{2-} (+, doubling time >10 h; ++, 6–10 h in low SO_4^{2-} medium); +++, growth on SO_4^{2-} is comparable to that of CP154-7B transformed with the unaltered *Sultr1;2* gene. Protein accumulation measurements are based on immunological signals from the fused C-terminal HA epitope relative to the Pma1 signal, as shown in Fig. 3: +, <20% of wild type; ++, between 20% and 70% of wild type; +++, >70% of wild type. Accumulation in the plasmamembrane is based on data presented in Fig. 4.

Mutation class	Codon change	Amino acid change	Location in STAS	Phenotype		
				Rescue of CP154-7B growth	Protein accumulation	Localization to plasmamembrane
I	1696 TCA>CCA	S546P	α1	−	+	−
	1777 CAG>CCG	Q573P	β3	−	+	+
	1791 ATC>AAC	I577N	β3	−	+	+
	1792 GAA>AAA, 1774 ATT>ATA (572I>I)	E578K	β3	−	+	+
	1879 TTG>TGG	L607W	β4	−	+	−
II	1546 ATC>ACC	I496N	L region	−	++	+
	1567 CCT>CTT	P503L	L region	−	+++	+
	1585 GGA>GAA	G509E	L region	−	+++	+
	1591 ATT>ACT	I511T	L region	−	+++	+
	1591 ATT>AAT	I511N	L region	−	++	+
	1609 TAC>TGT, 1663 ATT>ATC(I535I), 1723 AGA>AGG(R555R), 1906 GTG>GAG	Y517C, V616E	L region and α3	−	++	+
	1612 AGA>AGT	R518S	L region	−	++	+
	1624 CAG>AAG	Q522K	β1	−	+++	+
	1627 TAT>CAT	Y523H	β1	−	+++	+
	1669 GTT>GCT	V537A	β2	−	++	+
	1669 GTT>GAT	V537D	β2	−	+++	+
	1684 TAC>TGT	Y542C	α1	−	+++	+
	1687 TTC>TAC	F543Y	α1	−	+++	+
	1693 AAC>ATC,1801CCT>CCC(P581P), 1900 CCG>CCT(P614P)	N545I	α1	−	+++	+
	1822 AGT>AGA	S588R	α2	−	++	+
	1891AAT>AAA	N611K	Between β4 and α3	−	++	+
	1891 AAT>AGT	N611S	Between β4 and α3	−	++	+
III	1621 CAA>CTA	Q521L	L region	+++	+++	
	1705 GTT>TTT	V549F	α1	+	++	
	1738 GAA>GGA	E560G	α1	+	++	
	1909 ATA>ATG	I617M	α3	+++	+++	
	1948 GGA>GTA	G630V	Between α3 and α4	+	++	
	1672 GAC>GGC, 1708 AGA>GGA, 1909 ATA>ATG	D538G, R550G, I617M		+	++	
	1639 ACT>GCT, 1903 TTG>ATG, 1969 ACG>GCG, 1975GCT>GCA(A639A)	T527A, L615M, T637A		++	+++	
	1738 GAA>AAA, 1882 ATT>GTT, 1900 CCG>TCG	E560K, I608V, P614S		+	++	
	1678 GCC>TCC, 1705 GTT>ATT, 1882 ATT>GTT	A540S, V549I, I608V		++	++	

the transporter protein among the different cellular membrane fractions (Fig. 4). Transformants with low overall levels of Sultr1;2 polypeptide showed either no (S546P and L607W) or very low (V537D, V537A, Q573P, I577N, and E578K) accumulation in the plasmamembrane (Fig. 4, *fractions 10–13* from the gradient). In some cases (V537D, I577N, and L607W) a significant level of Sultr1;2 was observed in membrane fractions lighter than the plasmamembrane. These results demonstrate that some of the aberrant Sultr1;2 proteins cannot reach their site of function in the plasmamembrane (or reach it less efficiently, or the polypeptide is not stable once in the plasmamembrane), explaining their inability to rescue CP154-7B for methionine auxotrophy. However, the majority of transformants that were unable to grow with SO_4^{2-} as the sole S source (*e.g.* I496N, P503L, G509E, I511T, I511N, Y517C/V616E, R518S, Q522K, Y523H, V537A, Y542C, F543Y, N545I, V549F, S588R, N611K, N611S, and G630V) showed a relatively normal distribution of Sultr1;2 among the membrane fractions, with much of it being localized to the plasmamembrane. The Sultr1;2 proteins synthesized in these latter transformants (Class II) are likely to be defective for transport function.

Transformants Synthesizing Functional Sultr1;2—Transformants for which the mutated Sultr1;2 was able to rescue the methionine auxotrophy phenotype of the CP154-7B are listed in Table 1 as Class III. Some of these mutants had more than one lesion within the L-STAS region. The doubling time of these strains in both low and high SO_4^{2-} medium is presented in Fig. 2*B*. Relative accumulation of Sultr1;2 in these strains and their ability to take up SO_4^{2-} are shown in Fig. 5, *A* and *B*, respectively. We also calculated a K_m and V_{max} for the uptake of SO_4^{2-} by each strain, as shown in Table 2. Growth rates of individual strains varied and generally showed a positive correlation with the V_{max} for SO_4^{2-} uptake (Table 2; growth rate data are from Fig. 2*B*); the growth of E560G, which has a large standard deviation, is the only exception. The decreased rate of SO_4^{2-} uptake in many of the strains harboring functional *Sultr1;2* mutant alleles was mostly explained by decreased protein accumulation, with a few exceptions. T527A/L615M/T637A and A540S/V549I/I608N show decreased SO_4^{2-} uptake relative to WT′ (Fig. 5*B*), whereas protein accumulation (Fig. 5*A*) and distribution in plasmamembrane are comparable to that of WT′ (data not shown). V549F also shows very limited uptake; its V_{max} was 10% of WT′, whereas protein accumulation was approximately half of WT′.

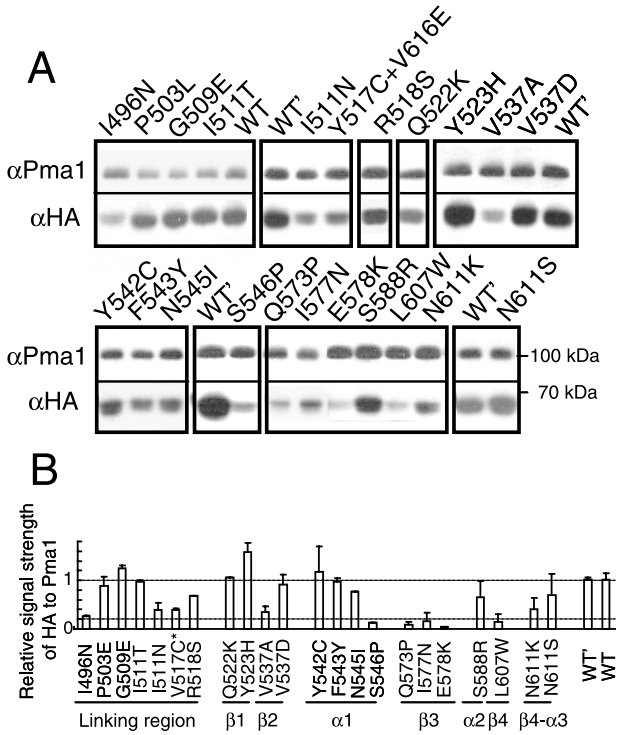

FIGURE 3. **Sultr1;2 protein levels in strains carrying mutant alleles of *Sultr1;2*.** *A*, lysates were prepared from CP154-7B expressing various mutated forms of Sultr1;2. The polypeptides of the lysates were resolved by SDS-PAGE, transferred to polyvinylidene difluoride membranes, and the Sultr1;2 and Pma1 proteins were detected using antibodies, as described under "Experimental Procedures." *B*, signal strengths of antibody reactions were quantified using Image J (National Institutes of Health, rsb.info.nih.gov/ij/), and those for Sultr1;2 (anti-HA antibodies) were normalized with respect to those for Pma1 (anti-Pma1 antibodies). *, allele "Y517C" also has a V616E substitution.

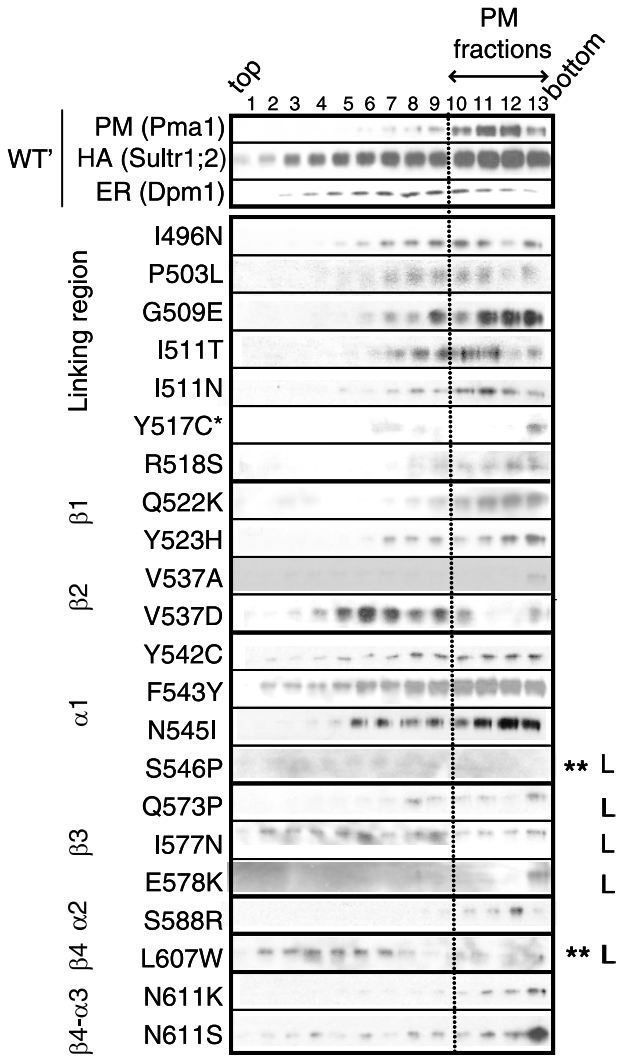

FIGURE 4. **Subcellular localization of mutant Sultr1;2 polypeptides.** Cell lysates (see "Experimental Procedures") were fractionated on 30–60% sucrose gradients, fractions were separated by SDS-PAGE, and Sultr1;2 immunodetected by anti-HA antibodies (*HA*). Distributions of the plasmamembrane marker Pma1 (*PM*) and the ER marker Dpm1 (*ER*) were visualized by Western blot analyses using monoclonal antibodies. The plasmamembrane was mainly in *fractions 10–13*. *, Tyr-517 allele also has a V616E mutation. The "*L*" indicates low accumulation of Sultr1;2 in whole cell extracts; **, no Sultr1;2 was detected in the plasmamembrane.

DISCUSSION

This study focused on determining residues of the L-STAS domain critical for biogenesis and functionality of Sultr1;2. We performed random mutagenesis of the *Sultr1;2* sequence encoding the L-STAS domain, replaced the unaltered L-STAS encoding region with a population of mutagenized L-STAS encoding regions, and identified lesions that resulted in both functional and nonfunctional Sultr1;2 polypeptides (Table 1 and Fig. 6). Among the alleles encoding nonfunctional Sultr1;2, some accumulated little protein (Class I), most of which was unable to properly integrate into the plasmamembrane, and others accumulated normal protein levels with seemingly proper plasmamembrane localization (Class II). We also identified alleles with lesions in the L-STAS domain that could complement the CP154-7B phenotype (Class III), although usually not fully restore the growth rate in low SO_4^{2-} medium.

To help interpret the effect of amino acid substitutions in mutated Sultr1;2, we used a STAS domain model, based on the SpoIIAA crystal structure (14). The STAS domain is thought to consist of four β-strands, forming a β-sheet, surrounded by five α-helices, as shown in Fig. 7. The β-sheet, in association with hydrophobic surfaces of the α-helices, forms a hydrophobic core that is not readily accessible to the external medium. In contrast, the externally exposed surfaces of the α-helices, and the loops between α-helices and β-strands, are predicted to be exposed and available for interactions with molecules in the solution environment. Although the L region was shown to be of importance for transporter function, it could not be modeled because it is not very similar to other known structures in the Protein Data Bank (PDB).

Mutations That Affect Biogenesis of Sultr1;2—β-Sheet—Class I mutations diminished Sultr1;2 protein accumulation in the plasmamembrane (surrounded by *blue boxes* in Fig. 6), and some Class III mutations decreased protein accumulation, with some activity still retained (surrounded by *black boxes* in Fig. 6). Interestingly, most of the lesions for which the protein shows little accumulation are in or immediately contiguous to β-strands 3 and 4 that are part of the β-sheet structure (Figs. 6 and 7); the mutations in or immediately adjacent to β1 and β2 were nonfunctional, but the protein accumulated in the plasmamembrane.

The Q573P, I577N, and E578K substitutions in β3 all alter the charge/hydrophobic character of the domain (Pro poten-

tially causes a kink in the polypeptide); polypeptides with these amino acid substitutions do not accumulate in CP154-7B (Fig. 3). As shown in the logo diagram (Fig. 6), Ile-577 and Glu-578 are highly conserved, whereas Gln-573 is not. Substitution of the conserved, hydrophobic Leu-607 to Trp in β4 also caused marked reduction in polypeptide accumulation (Fig. 3).

Some mutations predicted to be in the β-sheet vicinity, as shown in Fig. 7, also caused the polypeptide to accumulate to a lesser extent than WT′ Sultr1;2. Sultr1;2 with N611K or N611S (end of β4) substitution cannot rescue the CP154-7B phenotype. These strains exhibit a significant amount of protein accumulation (considered to be Class II), but lower than in WT, suggesting that the N611K/S lesions negatively affect protein biogenesis as well as transport function. Asn-611 is analogous to Asn-81 in SpoIIAA of *B. sphaericus*. The side chain of Asn-81 forms a hydrogen bond with Ala-102 in β5 in SpoIIAA, extending the β-sheet structure (22). Thus, Asn-611 of Sultr1;2 STAS may form an analogous hydrogen bond with Leu-636 (corresponds to Ala-102 in SpoIIAA) and thereby help stabilize the β-sheet structure of the polypeptide. CP154-7B transformed with Sultr1;2 with the G630V substitution (between α3 and α4, Class III), predicted to be in the region corresponding to β5 in SpoIIAA, exhibited reduced SO_4^{2-} uptake activity (Fig. 5*B*), which also correlated with reduced protein accumulation (Fig. 5*A* and Table 2), suggesting that the G630V substitution (*shaded gray* in Fig. 7) also affects protein biogenesis/turnover rather than function.

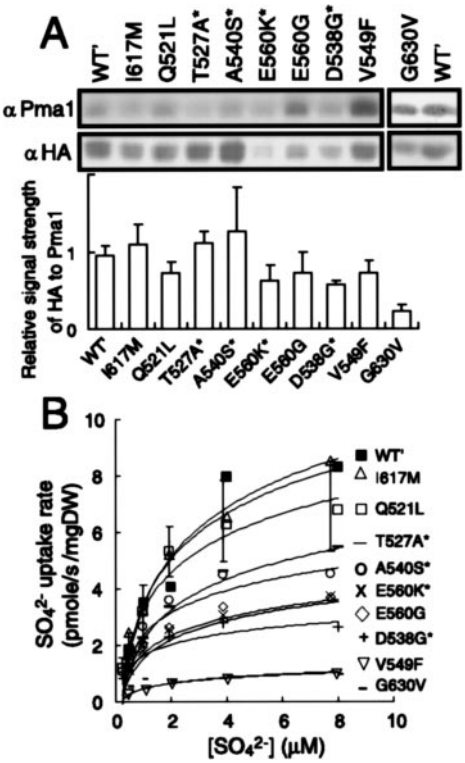

FIGURE 5. **Analysis of strains expressing functional Sultr1;2 in CP154-7B.** *A*, Sultr1;2 accumulation was determined in the same manner as described for Fig. 3. *B*, SO_4^{2-} uptake rates (see "Experimental Procedures") of CP154-7B expressing mutant and wild type (*WT′*) Sultr1;2 were determined. The uptake assay was performed with cells grown in SD-His-Met medium containing 500 μM SO_4^{2-} at an $A_{600} = 0.1 \sim 0.3$. The standard deviation for uptake values for all mutants was small, except for the Q521L strain, for which standard deviation values are shown. Mutant alleles marked with *asterisks* contain additional lesions. T527A* represents Sultr1;2 with the substitutions T527A, L615M, and T637A. Other alleles of *Sultr1;2* with multiple mutations are A540S* (A540S, V549I, and I608V); E560K* (E560K, I608V, and P614S); and D538G* (D538G, R550G, and I617M).

The L region do not significantly alter protein accumulation, Together, these findings demonstrate that lesions within or close to the STAS domain β-sheet of Sultr1;2 can significantly change protein stability or biogenesis. This appears to be especially true when the lesions are in β3 and β4. The β-sheet seems to serve as a core structure of the STAS domain and lesions within this structure may disrupt proper STAS packing, which could destabilize the entire Sultr1;2 polypeptide.

In addition, the V537A and V537D mutations, considered Class II, are in the C-terminal region of β2 (Fig. 6, surrounded by *purple boxes*); the former lesion did cause significant reduction in polypeptide accumulation, whereas the polypeptide level in the latter remained high (Fig. 3). The V537D substitution appears to result in a defect in plasmamembrane localization of Sultr1;2 (Fig. 4). These results suggest that Val-537 may be involved in the biogenesis of Sultr1;2 as well as transport function. Next to Val-537, a D538G substitution generated a Class III mutant; the Sultr1;2 protein accumulates to low levels in CP154-7B with low SO_4^{2-} transport activity. However, this allele has two other lesions, R550G (α1) and I617M (α3). The Sultr1;2 protein with a single I617M substitution accumulated in CP154-7B transformants to a level comparable to that of the unaltered protein and exhibited near normal levels of SO_4^{2-} transport activity. Thus D538G and/or R550G are likely to be responsible for the defect in protein biogenesis.

Other Destabilizing Lesions—Although most modifications of

TABLE 2

Phenotypes associated with Class III *Sultr1;2* alleles

V_{max} and K_m are based on data shown in Fig. 5*B*, relative protein accumulation is from Fig. 5*A*, and doubling time in low SO_4^{2-} liquid medium is from Fig. 2*B*. Standard deviations are in parentheses.

Amino acid change	K_m	V_{max}	Relative protein accumulation	Doubling time
	μM	*pmole/s/mg of DW*		*h*
WT′	2.7 (0.6)	11.5 (0.8)	1.0 (0.1)	5.6 (0.5)
I617M	2.4 (0.3)	10.8 (0.7)	1.1 (0.2)	6.5 (1.0)
Q521L	1.7 (0.5)	8.3 (2.1)	1.1 (0.3)	5.8 (0.6)
T527A, L615M, T637A	2.8 (0.3)	6.7 (2.4)	1.3 (0.6)	9.1 (2.0)
A540S, V549I, I608V	1.5 (0.7)	6.1 (1.9)	0.6 (0.1)	8.7 (2.5)
E560K, I608V, P614S	1.8 (0.4)	4.1 (2.0)	0.7 (0.3)	12.5 (3.2)
E560G	1.7 (0.8)	4.3 (0.5)	0.7 (0.2)	21.3 (9.3)
D538G, R550G, I617M	0.6 (0.1)	2.7 (0.2)	0.6 (0.2)	12.2 (2.5)
V549F	1.5 (0.1)	1.2 (0.2)	0.6 (0.2)	25.2 (6.6)
G630V	1.6 (0.4)	1.2 (0.1)	0.2 (0.1)	28.6 (9.8)

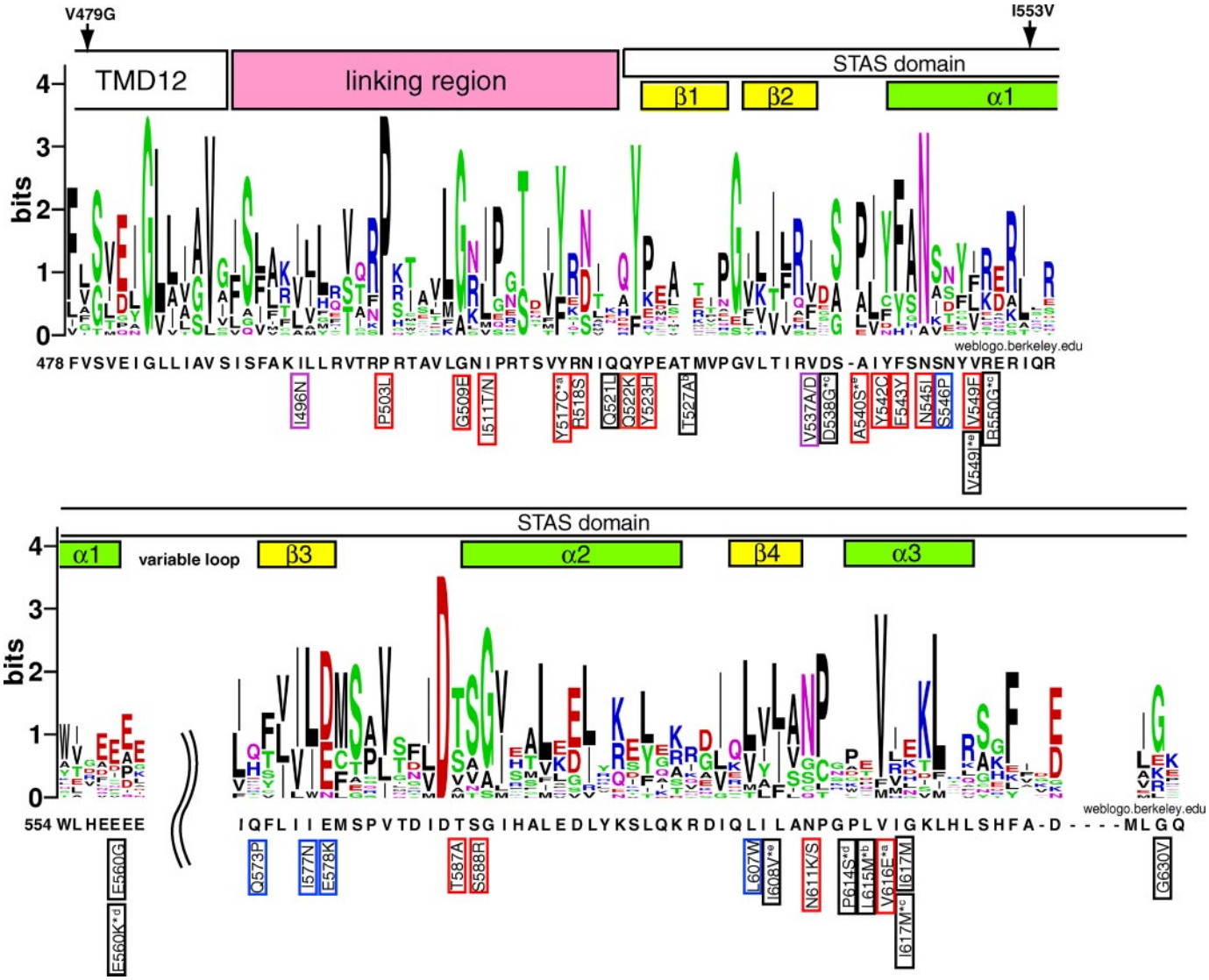

FIGURE 6. **Sequence logos representing residue frequencies.** Frequencies were determined using twelve *A. thaliana* sulfate transporters, five human SLC26 family members, and PDB code 1h4z (SpoIIAA). Features of the presentation were previously described (Ref. 24; available at weblogo.berkeley.edu/). The *y* axis indicates how often a particular amino acid is present at the location. Basic amino acids (*K*, *R*, and *H*) are *blue*, acidic amino acids (*D* and *E*) are *red*, polar amino acids (*G*, *S*, *T*, *Y*, and *C*) are *green*, *N* and *Q* are *purple*, and hydrophobic amino acids (*A*, *V*, *L*, *I*, *P*, *W*, *F*, and *M*) are *black*. Only amino acids with a certain degree of conservation are included in the output of the logo diagram. Unconserved amino acids do not appear in the output. The amino acid sequence of Sultr1;2 is below the sequence logos, and specific mutations analyzed are indicated below the Sultr1;2 sequence. *Blue boxes* mark nonfunctional Class I substitutions that cause a decrease in protein accumulation. *Red boxes* mark nonfunctional Class II substitutions that allow for high level protein accumulation, and proper localization of the protein to the plasmamembrane; exceptions are I496N and V537A/D (surrounded by *purple boxes*), which affect protein accumulation more severely than the other Class II lesions (see text). *Black boxes* mark Class III mutations, which often result in reduced protein accumulation, but the Sultr1;2 that remains confers some uptake activity to transformants. *Asterisks* indicate alleles with multiple mutations. *a*, allele V616E* has Y517C; *b*, allele T527A* has L615M and T637A; *c*, allele D538G* has R550G and I617M; *d*, allele P614S* has E560K and I608V; and *e*, allele I608V* has A540S and V549I. Two mutations introduced for cloning purposes during the construction of mutagenized library are also indicated (V479G and I553V).

the I496N lesion is a notable exception; this mutant polypeptide accumulates to ~25% of the level of unaltered Sultr1;2 (the lowest level among Class II mutant alleles), with some being localized to the plasmamembrane (Figs. 3 and 4). Hence, the L region may play some role in the biogenesis/stabilization of Sultr1;2. Recently, the motor protein prestin (SLC26A5), altered at a position corresponding to Ile-496 in Sultr1;2 (V499G in prestin), with an additional Y501H change, exhibited normal protein accumulation with diminished functionality (29). Position Ile-496 is represented by hydrophobic amino acids in most sulfate transporters (Fig. 6, I496N mutations are surrounded by a *purple box*).

The S546P substitution is the only Class I modification characterized that is in an α helix (Table 1). Introduction of a Pro residue in this α helix may cause extreme conformation perturbation by introducing steric constraints into the protein and disrupting the α1 structure, which in turn could lead to a marked decrease in protein accumulation. Furthermore, CP154-7B expressing Sultr1;2 with a E560G lesion exhibits slow growth and low rates of SO_4^{2-} uptake, which correlates with reduced protein accumulation (Table 2). These results suggest a potential role of Glu-560 in protein biogenesis/stability rather than in function (it is *shaded gray* in Fig. 7). Glu-560 is highly conserved among *A. thaliana* Sultr polypeptides and

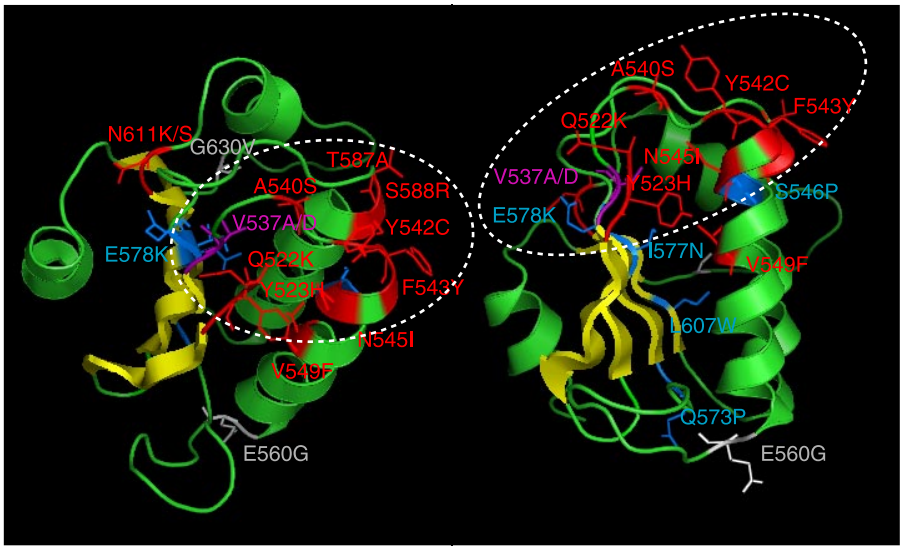

FIGURE 7. **Three-dimensional structural model of STAS domain of Sultr1;2 with mutations that affect its function.** These figures were generated using the program PyMol (pymol.sourceforge.net/), showing the three-dimensional structure of STAS domain based on the three-dimensional model reported by Rouached *et al.* (2005) from two different angles. β-Strands are colored *yellow*. The structures show side chains of the original residues substituted in mutant Sultr1;2 polypeptides. Coloring of the residues indicates the consequences of the substitution, as in Fig. 6. Note that E560G and G630V (substitutions in *gray*) cause decreased accumulation of the Sultr1;2 polypeptide, but the remaining protein exhibits some activity (suggesting that Glu-560 and Gly-630 are important in Sultr1;2 biogenesis). The mutations that allow Sultr1;2 protein accumulation but diminish its function are mostly clustered on the STAS surface, which is delimited in both STAS domain orientations shown by *dotted lines*. This surface includes Ala-540, Tyr-542, Phe-543, and Asn-545, which are in or contiguous to the N terminus of α1, Thr-587 and Ser-588 in the N-terminal end of α2, Gln-522 and Tyr-523 in the N-terminal end of β1, and Val-537 in the C-terminal end of β2.

part of an acidic cluster located at the C-terminal end of α1, or possibly at the beginning of the variable loop (2).

Mutations That Affect Activity of Sultr1;2 but Not Biogenesis—Class II mutations are defined as lesions that eliminate the functionality of Sultr1;2, although the aberrant polypeptide accumulates to relatively normal levels in the plasmamembrane (surrounded by *red boxes* in Fig. 6). These lesions are mostly in the L region and the protein surface formed by the N termini of α-helices and some contiguous sequences. These subdomains appear to be crucial for maintaining transporter activity.

L Region—Most of the lesions in the L region of Sultr1;2, including P503L, G509E, I511T, I511N, Y517C/V616E, and R518S, caused little change in either protein abundance or plasmamembrane localization, suggesting an involvement of the L region in sulfate transporter function and not biogenesis. All of these positions are highly conserved among SLC26 family members. Pro-503 is in a predicted loop that may separate two β-strands or a β-strand and α-helix, based on various algorithms used for protein structure predictions (PELE Protein Structure Prediction at workbench.sdsc.edu) and is fully conserved in SLC26 family members (Fig. 6). This Pro may undergo cis-trans isomerization, which may specify the physical distance between the catalytic moiety of the transporter and the STAS domain to, in some unknown way, regulate transport activity. Substitution by a Leu would markedly change this distance.

Specific STAS Surface Critical for Activity—Sultr1;2 with individual Y542C, F543Y, or N545I substitutions appeared completely nonfunctional, even though there was normal accumulation of the polypeptide in the plasmamembrane (Figs. 2–4). These residues are located in the N terminus of α1 and the loop adjacent to α1 (Figs. 6 and 7), regions that are well conserved in transporters of the SLC26 family (Fig. 6). It is noteworthy that a Cys is observed at the position analogous to Tyr-542 of Sultr1;2 only in low affinity type sulfate transporters (Sultr2;1 and Sultr2;2), and a Tyr at the position analogous to Phe-543 of Sultr1;2 in human SLC26A proteins, but not in those of plants (Fig. 7). This suggests strict Tyr and Phe requirements at these positions in some SLC26 transporter sub-types. In addition, Sultr1;2 with three amino acid substitutions, A540S, V549I, and I608V, accumulates to normal levels in transformed CP154-7B but has reduced SO_4^{2-} uptake activity (Fig. 5 and Table 2, Class III). Although it is not known which among the three substitutions leads to reduced transport activity, A540S is most likely to have the greatest effect on the structure/function of the polypeptide, because the V549I and I608V substitutions are likely to have little effect on protein structure/activity: they have highly similar character to Val and Ile (therefore, a *red box* was placed around A540S in Fig. 6). Position 540 is occupied by a nonpolar amino acid (Pro, Ala, or Leu) in most SLC26 family members (Fig. 6). Substitution by Ser, which is polar, may disturb molecular interactions required for function. The results presented above suggest that the N terminus of α1 plus the adjacent loop are critical for maintaining Sultr1;2 function (not accumulation or localization). This conclusion is also supported by the finding that the I544N allele of human DRA (HCO_3^--Cl^- exchanger) is functionally inactive and causes congenital chloride diarrhea (15, 30); Ile-544 in human DRA corresponds to Ile-541 in Sultr1;2.

The polypeptide surface defined by the N terminus of α1 can be extended toward the top end of the β-sheet structure and the N terminus of α2. These regions also contain Class II lesions, and the side chains of all of these residues are in close proximity in the three-dimensional structural model (delimited by *dotted lines* in Fig. 7). The Q522K and Y523H substitutions, at the N terminus of β1 (Fig. 6), result in accumulation of nonfunctional Sultr1;2 in the plasmamembrane (Figs. 3 and 4). Sultr1;2 with V537A/D (C-terminal end of β2) or S588R mutations (N-terminal end of α2) are also nonfunctional; these mutant proteins accumulate in cells to a somewhat lower level than the WT′ protein (Figs. 3 and 4). A T587A substitution (potentially a phosphorylation site) was previously shown to eliminate Sultr1;2 activity and is a potential site of phosphorylation (14). The Ser-588, Thr-587, and Asp-586 side chains have the potential to form charge-dipoles, similar to the interactions demonstrated for SpoIIAA (22).

Overall consideration of the polypeptide structure predicts that residues Gln-522, Tyr-523, Val-537, Ala-540, Tyr-542,

Phe-543, Asn-545, Thr-587, and Ser-588 are located on the same STAS surface (see Fig. 7). Hence, lesions on this surface appear to generate a protein with severely compromised function. This STAS surface is analogous to a region of SpoIIAA that allows SpoIIAB binding and subsequent SpoIIAA phosphorylation (31). Although there is no evidence of phosphorylation of STAS domains of SLC26A family proteins, accumulation of critical amino acid residues along the STAS surface associated with protein interactions in SpoIIAA raises the possibility of molecular interactions that affect sulfate transporter activity in this analogous STAS sub-domain. Recently, preliminary results have demonstrated an interaction between L-STAS regions (these regions appear to form a homomeric oligomer), and that both the L and the STAS domains are involved in this interaction; more work is required to determine the precise requirements for this interaction.

Furthermore, there seems to be a requirement for a Val at position 549 of Sultr1;2, because the V549F substitution (toward the middle of α1) shows only residual transporter activity, although the protein accumulates to nearly the same extent as the WT′ protein (Fig. 5) and is localized in the plasmamembrane (data not shown). A substitution by Phe, another hydrophobic amino acid, but with a bulky side chain, causes a loss of activity. Interestingly, Phe is present at this position in some human but not in plant SLC26A proteins (Fig. 6). Examination of the predicted three-dimensional structure of the Sultr1;2 STAS domain suggests that Val-549 is either part of or contiguous to the putative interacting surface discussed above (see Fig. 7) and that a V549F substitution may distort the surface, compromising specific interactions.

The results for some mutated proteins are more difficult to interpret because of the presence of multiple lesions. The T527A(β1) plus L615M(α3) plus T637A (between α3 and α4) strain accumulates Sultr1;2 to approximately the same level as that of WT′ but has ~30% lower SO_4^{2-} uptake activity (Fig. 5), suggesting that none of these changes significantly alters Sultr1;2 biogenesis but that they have some effect on transport function.

Lesions That Do Not Affect Biogenesis or Function—Although Class III mutations were identified to find residues of the STAS domain that were not essential residues for Sultr1;2 activity, most mutations in this class decreased protein accumulation and/or function to some extent, except for Q521L and I617M. Sultr1;2 with a Q521L or I617M substitution rescued the CP154-7B growth (Fig. 2) and SO_4^{2-} transport (Fig. 5*B* and Table 2) phenotypes to the same extent as WT′. Gln-521 is at the most C-terminal residue of the L region, Ile-617 is in α3, and neither of them is highly conserved among family members (Fig. 6, mutations surrounded by *black boxes*). These results suggest that there is no absolute requirement for Gln and Ile at these positions. Other mutations identified within α3 include P614S, L615M, and V616E (Fig. 6). Because the alleles with these mutations all contain other lesions, definitive conclusions on the importance of α3 are difficult to draw at this time.

REFERENCES

1. Mount, D. B., and Romero, M. F. (2004) *Pflugers Arch.* **447,** 710–721
2. Aravind, L., and Koonin, E. V. (2000) *Curr. Biol.* **10,** R53–R55
3. Zheng, J., Long, K. B., Shen, W., Madison, L. D., and Dallos, P. (2001) *Neuroreport* **12,** 1929–1935
4. Lohi, H., Lamprecht, G., Markovich, D., Heil, A., Kujala, M., Seidler, U., and Kere, J. (2003) *Am. J. Physiol.* **284,** C769–C779
5. Ho, M. S., Carniol, K., and Losick, R. (2003) *J. Biol. Chem.* **278,** 20898–20905
6. Crosson, S., Rajagopal, S., and Moffat, K. (2003) *Biochemistry* **42,** 2–10
7. Superti-Furga, A., Rossi, A., Steinmann, B., and Gitzelmann, R. (1996) *Am. J. Med. Genet.* **63,** 144–147
8. Hastbacka, J., Superti-Furga, A., Wilcox, W. R., Rimoin, D. L., Cohn, D. H., and Lander, E. S. (1996) *Ann. N. Y. Acad. Sci.* **785,** 131–136
9. Everett, L. A., Glaser, B., Beck, J. C., Idol, J. R., Buchs, A., Heyman, M., Adawi, F., Hazani, E., Nassir, E., Baxevanis, A. D., Sheffield, V. C., and Green, E. D. (1997) *Nat. Genet.* **17,** 411–422
10. Usami, S., Abe, S., Weston, M. D., Shinkawa, H., Van Camp, G., and Kimberling, W. J. (1999) *Hum. Genet.* **104,** 188–192
11. Everett, L. A., and Green, E. D. (1999) *Hum. Mol. Genet.* **8,** 1883–1891
12. Ko, S. B., Shcheynikov, N., Choi, J. Y., Luo, X., Ishibashi, K., Thomas, P. J., Kim, J. Y., Kim, K. H., Lee, M. G., Naruse, S., and Muallem, S. (2002) *EMBO J.* **21,** 5662–5672
13. Shibagaki, N., and Grossman, A. R. (2004) *J. Biol. Chem.* **279,** 30791–30799
14. Rouached, H., Berthomieu, P., El Kassis, E., Cathala, N., Catherinot, V., Labesse, G., Davidian, J. C., and Fourcroy, P. (2005) *J. Biol. Chem.* **280,** 15976–15983
15. Chernova, M. N., Jiang, L., Shmukler, B. E., Schweinfest, C. W., Blanco, P., Freedman, S. D., Stewart, A. K., and Alper, S. L. (2003) *J. Physiol.* **549,** 3–19
16. Ko, S. B., Zeng, W., Dorwart, M. R., Luo, X., Kim, K. H., Millen, L., Goto, H., Naruse, S., Soyombo, A., Thomas, P. J., and Muallem, S. (2004) *Nat. Cell Biol.* **6,** 343–350
17. Takahashi, H., Yamazaki, M., Sasakura, N., Watanabe, A., Leustek, T., de Almeida Engler, J., Engler, G., Van Montagu, M., and Saito, K. (1997) *Proc. Natl. Acad. Sci. U. S. A.* **94,** 11102–11107
18. Takahashi, H., Watanabe-Takahashi, A., Smith, F., Blake-Kalff, M., Hawkesford, M. J., and Saito, K. (2000) *Plant J.* **23,** 171–182
19. Smith, F. W., Hawkesford, M. J., Ealing, P. M., Clarkson, D. T., Vanden Berg, P. J., Belcher, A. R., and Warrilow, A. G. (1997) *Plant J.* **12,** 875–884
20. Vidmar, J. J., Schjoerring, J. K., Touraine, B., and Glass, A. D. M. (1999) *Plant Mol. Biol.* **40,** 883–892
21. Cherest, H., Davidian, J.-C., Thomas, D., Benes, V., Ansorge, W., and Surdin-Kerjan, Y. (1997) *Genetics* **145,** 627–637
22. Seavers, P. R., Lewis, R. J., Brannigan, J. A., Verschueren, K. H., Murshudov, G. N., and Wilkinson, A. J. (2001) *Structure* (*Camb*) **9,** 605–614
23. Burke, D., Dawson, D., and Stearns, T. (2000) *Methods in Yeast Genetics*, pp. 103–105, Cold Spring Harbor Press, Plainview, NY
24. Crooks, G. E., Hon, G., Chandonia, J. M., and Brenner, S. E. (2004) *Genome Res.* **14,** 1188–1190
25. Cadwell, R. C., and Joyce, G. F. (1992) *PCR Methods Appl.* **2,** 28–33
26. Leung, D. W., Ellson, C., and Goeddel, D. V. (1989) *Techniques* **1,** 11–15
27. Shibagaki, N., Rose, A., McDermott, J. P., Fujiwara, T., Hayashi, H., Yoneyama, T., and Davies, J. P. (2002) *Plant J.* **29,** 475–486
28. Karniski, L. P. (2004) *Hum. Mol. Genet.* **13,** 2165–2171
29. Zheng, J., Du, G. G., Matsuda, K., Orem, A., Aguinaga, S., Deak, L., Navarrete, E., Madison, L. D., and Dallos, P. (2005) *J. Cell Sci.* **118,** 2987–2996
30. Hoglund, P., Sormaala, M., Haila, S., Socha, J., Rajaram, U., Scheurlen, W., Sinaasappel, M., de Jonge, H., Holmberg, C., Yoshikawa, H., and Kere, J. (2001) *Hum. Mutat.* **18,** 233–242
31. Masuda, S., Murakami, K. S., Wang, S., Anders Olson, C., Donigian, J., Leon, F., Darst, S. A., and Campbell, E. A. (2004) *J. Mol. Biol.* **340,** 941–956